Theor Chem Acc (1998) 100:117–123
DOI 10.1007/s002149800m38

Theoretical
Chemistry Accounts

Regular article

Calculation of ground- and excited-state potential energy curves for barium-rare gas complexes in a pseudopotential approach*

E. Czuchaj[1], F. Rebentrost[1], H. Stoll[2], H. Preuss[2]

[1]Max-Planck-Institut für Quantenoptik, D-85748 Garching near Munich, Germany
[2]Institut für Theoretische Chemie, Universität Stuttgart, Pfaffenwaldring 55, D-70550 Stuttgart, Germany

Received: 7 April 1998 / Accepted: 27 July 1998 / Published online: 12 October 1998

Abstract. Adiabatic potential curves for the ground state and several low-lying excited states of the barium atom interacting with Ne, Ar, Kr and Xe have been obtained from valence ab initio configuration-interaction calculations. Atomic cores are replaced by scalar-relativistic *l*-dependent pseudopotentials, while core-polarization potentials are used for describing correlation contributions of the rare-gas atoms and the Ba^{2+} cores. Implications of the resulting potential curves for the interpretation of experimental data are discussed, together with first applications of the curves for calculating absorption profiles of the $(6s^2)^1S \rightarrow (6p)^1P$ Ba transition.

Key words: Collision complexes – Pseudopotential method – Potential curves

1 Introduction

Experimental and theoretical investigations of atomic collision processes are attracting the interest of a growing number of researchers. These studies are mainly inspired by a desire to obtain information about collisional mechanisms and interaction potentials governing the atomic collisions. Processes such as fine-structure-changing collisions, electronic-to-vibrational energy transfer, charge-transfer collisions, energy-pooling collisions and spin-changing collisions have been investigated in many laboratories. Some of these processes were first studied in alkali atoms undergoing collisions with a buffer gas. Owing to the presence of three possible fine-structure-changing transitions and spin-changing transitions, the collisional processes in alkaline earth atoms possess a much greater richness and complexity than those in alkali atoms. For the alkaline earth atoms, the majority of experiments has been done for Ca, Sr and Ba. In particular, for the barium atom, pressure-broadening effects were measured, among others, by Kielkopf [1], Harima et al. [2], Ehrlacher and Huennekens [3, 4] and Kanorsky et al. [5], spin-changing collisions were studied by Breckenridge and Merrow [6] and Visticot et al. [7] and polarization effects were investigated by Alford et al. [8], Visticot et al. [9] and Ni et al. [10]. Excitation transfer among low-lying excited states of the Ba atom induced by collisions with rare gas (RG) atoms were studied by Ehrlacher and Huennekens [11], Vadla et al. [12] and Brust and Gallagher [13]. Diffusion of the ground- and lowest ^3D_j metastable-state barium atoms in a buffer gas was measured by Namiotka et al. [14]. Contrary to numerous experiments conducted on the barium-RG diatomics, only a few calculations have been performed for the appropriate collisional cross-sections [15, 16]. The reason for this is that a detailed theoretical treatment of collision processes requires a knowledge of reliable potential energy curves which, unfortunately, for the alkaline earth-RG pairs are still poorly known. The first attempt to calculate the singlet potential curves for the Ba-RG systems was undertaken by Czuchaj et al. [17]. Both singlet and triplet potential curves for Ba-He have so far been calculated by Czuchaj et al. [18] and Brust and Greene [19].

The adiabatic potential curves calculated by us for Ba-He have already been used successfully in evaluating excitation line profiles of the $^1S_0 \rightarrow {}^1P_1$ transition of barium in liquid helium at various pressures [5] and close-coupling calculations for the $Ba(6p\,{}^3P_j \leftarrow 6p\,{}^1P_1)$ excitation transfer and $Ba(6p\,{}^3P_{j\rightarrow j'})$ intramultiplet transition cross-sections in collisions with He [15]. In addition, the quality of the potentials has also been supported by recent calculations of the diffusion cross-section for ground- and $(5d)^3D_j$ metastable-state barium atoms in helium buffer gas [14]. Encouraged by these results we have decided to extend the calculations to the remaining Ba-RG pairs. Since fully ab initio calculations of molecular structure still require high computational effort for atoms as heavy as barium, an approach in which only the valence electrons of the interacting atoms are treated explicitly is justified. This allows us to use the

* Dedicated to Prof. Dr. Wilfried Meyer on the occasion of his 60th birthday

Correspondence to: E. Czuchaj, Institute of Theoretical Physics and Astrophysics, University of Gdańsk, ul. Wita Stwosza 57, PL 80-952 Gdańsk, Poland

pseudopotential method which is well documented in the literature. Moreover, relativistic effects which are important for heavy atoms like Ba can easily be incorporated in this way. In the present approach, the atomic cores are simulated by scalar-relativistic l-dependent energy-consistent pseudopotentials. Core-valence correlation effects are described by polarization potentials included in the effective molecular Hamiltonian. A configuration interaction (CI) treatment accounts for valence correlation effects and for the coupling between valence and core-valence correlation.

This paper presents the results of our pseudopotential CI calculations for the ground- and several excited-state potential energy curves of the Ba-Ne (Ar, Kr, Xe) complexes, at a scalar-relativistic level, i.e. without taking into account spin-orbit coupling. The calculated dipole moments for the transitions between the ground state and two lowest singlet excited states are also discussed. A brief summary of the method is given in Sect. 2. Details of the calculations are described in Sect. 3. The results and their discussion are presented in Sect. 4.

2 Method

The calculation of the adiabatic energies $E_i(R)$ between an alkaline earth atom (A) and a RG atom (B) in the Born-Oppenheimer approximation reduces to the solution of the Schrödinger equation

$$(H_A + H_B + V_{AB})\Psi_i(\mathbf{x}, \mathbf{R}) = E_i(R)\Psi_i(\mathbf{x}, \mathbf{R}) \tag{1}$$

where H_A and H_B are the Hamiltonians of the isolated atoms A and B, V_{AB} stands for the interaction between the two atoms, $\mathbf{x}$ represents the electronic coordinates, while $\mathbf{R}$ is the position vector of B relative to A. In the present approach only the valence electrons of the system are treated explicitly. The atomic cores are represented by l-dependent pseudopotentials. Consequently the total Hamiltonian in Eq. (1) can be expressed as $H = T + V$, where T stands for the kinetic energy operator of the valence electrons and V represents the interaction operator. The latter is put into the form

$$V = \sum_{\lambda}(V^{\lambda} + V^{\lambda}_{\mathrm{pol}}) + \sum_{j>i=1}^{N}\frac{1}{r_{ij}} + V_{\mathrm{cc}} \tag{2}$$

Here V^{λ} describes Coulomb and exchange interaction as well as the Pauli repulsion between the valence electrons and core λ and is defined as

$$V^{\lambda} = \sum_{i=1}^{N}\left(-\frac{Q_{\lambda}}{r_{\lambda i}} + \sum_{l,k} B^{\lambda}_{l,k}\exp(-\beta^{\lambda}_{l,k}r^2_{\lambda i})P^{\lambda}_{l}\right) \tag{3}$$

where Q_{λ} denotes the net charge of core λ, P^{λ}_{l} is the projection operator onto the Hilbert subspace of angular symmetry l with respect to core λ

$$P^{\lambda}_{l} = \sum_{m=-l}^{l}|\lambda lm\rangle\langle\lambda lm| \tag{4}$$

and N is the number of valence electrons. The parameters $B^{\lambda}_{l,k}$ and $\beta^{\lambda}_{l,k}$ define the semi-local energy-consistent pseudopotentials.

The second interaction term in Eq. (2) is the polarization term which describes, among others, core-valence correlation effects [20] and, in the case of atom A, is taken as

$$V^{\mathrm{A}}_{\mathrm{pol}} = -\frac{1}{2}\alpha_{\mathrm{A}}\mathbf{F}^2_{\mathrm{A}} \tag{5}$$

where α_{A} is the dipole polarizability of the A^{2+} core and $\mathbf{F}_{\mathrm{A}}$ is the electric field generated at its site by the valence electrons and the other (RG) core

$$\mathbf{F}_{\mathrm{A}} = \sum_{i}\frac{\mathbf{r}_{\mathrm{A}i}}{r^3_{\mathrm{A}i}}[1 - \exp(-\delta_{\mathrm{A}}r^2_{\mathrm{A}i})] - \frac{Q_{\mathrm{B}}\mathbf{R}}{R^3}[1 - \exp(-\delta_{\mathrm{A}}R^2)] \tag{6}$$

The cutoff parameter δ_{A} is effective only for short internuclear distances. Note that the polarization term consists not only of a simple one-electron potential but also of so-called cross terms. The inclusion of the cross terms is necessary if the model is to predict correctly the van der Waals-like interaction in the case of neutral species (cf. below). The third term in Eq. (2) represents the Coulomb repulsion between the valence electrons, whereas the last term describes the core–core interaction. Since the RG^{8+} and Ba^{2+} cores are well separated, we choose a simple point-charge Coulomb interaction in the latter case. As just indicated, the barium and RG atoms are treated as two- and eight-valence-electron systems, respectively. The RG orbitals are obtained first by performing a SCF calculation on the ground state of the RG atom. In the molecular calculations, the valence electrons of the RG atom remain frozen in their ground-state Hartree-Fock form. Such a frozen atom cannot, however, relax in the field produced by the alkaline earth atom. In order to account for polarization and correlation effects, the frozen RG atom is supplied with the static dipole (α_{dB}) and quadrupole (α_{qB}) polarizabilities along with the dynamical correction $\beta_{1\mathrm{B}}$. The one-electron part of the polarization potential localized on the RG atom is of the form

$$V^{\mathrm{B}}_{\mathrm{pol,e}}(r_{\mathrm{B}}) = -\frac{\alpha_{\mathrm{dB}}}{2r^4_{\mathrm{B}}}\omega^4(r_{\mathrm{B}}) - \frac{\alpha'_{\mathrm{qB}}}{2r^6_{\mathrm{B}}}\omega^6(r_{\mathrm{B}}) \tag{7}$$

where $\omega(x) = 1 - \exp(-\delta_{\mathrm{B}}x^2)$ defines the cutoff function with the cutoff parameter δ_{B} and $\alpha'_{\mathrm{qB}} = \alpha_{\mathrm{qB}} - 6\beta_{1\mathrm{B}}$. The associating cross-term which arises from the simultaneous polarization of the RG atom by the barium valence electrons and the net charge of the barium core is given by

$$V^{\mathrm{B}}_{\mathrm{pol,ec}}(\mathbf{r}_{\mathrm{B}}, \mathbf{R}) = Q_{\mathrm{A}}\alpha_{\mathrm{dB}}\frac{P_1(\cos\vartheta)}{R^2r^2_{\mathrm{B}}}\omega^2(r_{\mathrm{B}})\omega^2(R) + Q_{\mathrm{A}}\alpha_{\mathrm{qB}}\frac{P_2(\cos\vartheta)}{R^3r^3_{\mathrm{B}}}\omega^3(r_B)\omega^3(R) \tag{8}$$

where P_1 and P_2 are Legendre polynomials, ϑ is the angle between the vectors $\mathbf{r}_{\mathrm{B}}$ and $-\mathbf{R}$, and $Q_{\mathrm{A}} = 2$. Correspondingly, the cross-term resulting from the simultaneous polarization of the RG atom by the two Ba electrons is

$$V^{\mathrm{B}}_{\mathrm{pol,ee}}(\mathbf{r}_{\mathrm{B1}}, \mathbf{r}_{\mathrm{B2}}) = -\alpha_{\mathrm{dB}}\frac{P_1(\cos\vartheta_{12})}{r^2_{\mathrm{B1}}r^2_{\mathrm{B2}}}\omega^2(r_{\mathrm{B1}})\omega^2(r_{\mathrm{B2}}) - \alpha_{\mathrm{qB}}\frac{P_2(\cos\vartheta_{12})}{r^3_{\mathrm{B1}}r^3_{\mathrm{B2}}}\omega^3(r_{\mathrm{B1}})\omega^3(r_{\mathrm{B2}}) \tag{9}$$

where ϑ_{12} is the angle between the vectors $\mathbf{r}_{\mathrm{B1}}$ and $\mathbf{r}_{\mathrm{B2}}$.

3 Details of calculations

The parameters of the semi-empirical pseudopotential of barium are taken from Fuentealba et al. [21]. They were determined by adjusting the calculated energy levels for s, p and d symmetries of the BaII ion to the corresponding experimental energies [22]. In turn, the ab initio pseudopotential parameters for the RG atoms are taken from Nicklass et al. [23]. These energy-consistent pseudopotentials were determined with a multi-electron fit (MEFIT) procedure using quasirelativistic Wood-Boring all-electron reference data. The numerical values of the pseudopotential parameters for Ba as well as the parameters defining the polarization potential of the RG atoms are compiled in Table 1. The calculations were carried out employing Gaussian basis sets centred at each of the two atoms constituting the diatomic. The contracted $(9s7p5d)/(8s7p5d)$ basis set for Ba with the

exponents 2.187 (0.006185), 0.729 (0.132361), 0.243, 0.152, 0.036, 0.018, 0.009, 0.006 and 0.003 for *s* symmetry, 0.729, 0.243, 0.060, 0.030, 0.020, 0.008 and 0.04 for *p* symmetry and 1.0, 0.3, 0.1, 0.03 and 0.01 for *d* symmetry is slightly enlarged and modified compared with the basis set used in our earlier calculations [17]. Numbers in parentheses give the corresponding contraction coefficients. The calculated valence CI ionization energies (including the core- polarization potential) for the barium atom reproduce the experimental energy levels for several lowest terms quite well. We obtain (in atomic units) 0.559558 (0.559150), 0.503483 (0.507229), 0.479020 (0.476862), 0.514025 (0.516515) and 0.499860 (0.499538) for the $(6s^2)^1$S, $(6s5d)^1$D, $(6s6p)^1$P, $(6s5d)^3$D, and $(6s6p)^3$P Ba terms, respectively. Numbers in parentheses give the corresponding experimental ionization energies [22]. The exponential parameters of *s* and *p* symmetry of primitive basis sets for the RG atoms were taken from Nicklass et al. [23]. They were supplemented with a few diffuse exponents determined by means of even-tempered continuation of the series of low exponents to improve the description in the valence space; we added 0.118287, 0.045462 and 0.017472 (*s* symmetry) and 0.087244 (*p* symmetry) for Ne, 0.057726 and 0.025359 (*s* symmetry) and 0.039397 (*p* symmetry) for Ar and 0.065356, 0.024811 and 0.009419 (*s* symmetry) and 0.041501 (*p* symmetry) for Kr. In addition, for the same reason these basis sets were augmented by five *d* functions; we took 2.542082, 1.033764, 0.418788, 0.164627 and 0.064715 for Ne, 1.211516, 0.538499, 0.229575, 0.095103 and 0.039397 for Ar and 1.688360, 0.737900, 0.322500, 0.140900 and 0.061559 for Kr. The final basis sets are (10*s*8*p*5*d*)/[7*s*6*p*5*d*], (8*s*7*p*5*d*)/[7*s*6*p*5*d*] and (9*s*7*p*5*d*)/[7*s*6*p*5*d*], respectively, for Ne, Ar and Kr. For the Xe atom we also prepared a primitive (9*s*8*p*5*d*) set, but adopted the energy-optimized (6*s*6*p*1*d*)/[4*s*4*p*1*d*] basis set from [23] without further modifications, in the frozen-core calculations for the neutral systems; cf. below.

The present calculations were performed according to the following general procedure. First, CI calculations with all single and double substitutions (SD-CI) were carried out for the ground-state energy of the Ba^{2+}-RG systems. The ionic diatomic is here treated as an eight-electron system with the only valence electrons of the RG atom considered explicitly, whereas the barium ion is represented by the *l*-dependent pseudopotential along with the polarization term. In these calculations the uncontracted basis sets, as stated above, were used for all the RG atoms. Having calculated the SD-CI ground-state potential for the ionic diatomic, the RG atom is frozen in its Hartree-Fock ground-state configuration, with orbitals taken from atomic calculations, and the polarization potential given by Eqs. (7–9) is added to the molecular Hamiltonian. The cutoff parameter for the RG atom is determined by adjusting the SCF ground-state potential of the molecular ion calculated with the forzen RG atom to the earlier obtained SD-CI potential. The values of the cut-off parameter δ_B found in this manner are given in Table 1. The evaluated ground-state dissociation energies and equilibrium positions of the ionic diatomics are $D_e = 1650$ cm^{-1} and $R_e = 5.05$ bohr for Ba^{2+}-Ne, $D_e = 3050$ cm^{-1} and $R_e = 5.9$ bohr for Ba^{2+}-Ar, $D_e = 3822$ cm^{-1} and $R_e = 6.2$ bohr for Ba^{2+}-Kr, $D_e = 4355$ cm^{-1} and $R_e = 6.8$ bohr for Ba^{2+}-Xe. Second, having established the cut-off parameter δ_B, molecular calculations are performed for the neutral Ba-RG systems. Now the two valence electrons of Ba are active, whereas the RG electrons remain frozen throughout the calculations, static and dynamic polarization of the latter being accounted for by V_{pol}^B. The potential energies for the Ba-RG pair are obtained as a result of a 10-electron SCF calculation followed by a restricted CI calculation which includes all single and double excitations from the Ba doubly occupied $6s\sigma$ valence orbital. In addition, the CI space is generated only by the Ba basis functions since the RG basis remains fully contracted. In consequence the basis set superposition error could be neglected in the present considerations. It is essential that the calculated potentials are obtained without adjustment to any experimental data concerning the Ba-RG quasimolecule. Owing to that, the calculated interaction energies may be considered as an independent source of information on the investigated systems. The calculations were performed using the MELD program [24] installed on the CRAY-YMP supercomputer at Garching. Since the MELD program does not allow for spin–orbit coupling in the calculations explicitly, this effect has not been considered in the present work. However, the calculated potential curves could be easily split up into fine-structure components using the semiempirical approach of Cohen and Schneider [25], as was done by us earlier for Ba-He [18].

4 Results and discussion

Molecular-structure calculations have been performed for the internuclear separations ranging from 3.5 (4.0, 4.5 and 4.75) to 30 bohr, respectively, for Ba-Ne (Ar, Kr and Xe) with different step sizes. The atomic basis sets

Table 1. Pseudopotential parameters (au) for Ba and parameters defining the polarization potential on Ne, Ar, Kr and Xe

Element	α_A/α_{dB}	α_{qB}	β_{1B}	δ_A/δ_B	l	k	$B_{l,k}$	$\beta_{l,k}$
Ba	10.17			0.235	0	1	16.710	0.6356
					1	1	4.874	0.3214
					2	1	−0.8427	0.2403
Ne	2.663[a]	6.458[b]	1.27[c]	0.106				
Ar	11.0834[d]	48.237[e]	8.33[c]	0.079				
Kr	16.736[d]	78.762[e]	14.5[c]	0.077				
Xe	27.292[d]	128.255[e]	29.2[c]	0.071				

[a] [28]
[b] [29]
[c] [30]
[d] [31]
[e] [32]

were kept constant for all values of R. The potential energies were obtained by subtracting the asymptotic energy of the diatomic calculated at $R = 200$ bohr from the associated molecular energy at a given internuclear separation. The calculations involve the ground state and excited states up to that correlating with the $(6p)^1$P Ba term. The precision of our calculations can only be estimated by comparison with the available spectroscopic data and possible ab initio results. The calculated potentials are shown in Figs. 1–4 and their numerical values are available from the authors (E.C.) upon request. As seen from the figures, the corresponding potential curves belonging to different Ba-RG diatomics are very similar in shape. All potentials exhibit a repulsive character with shallow van der Waals minima at larger internuclear separations. The $(6p)^1\Sigma$ and $(6p)^3\Sigma$ potential curves for all the Ba-RG systems except for Ba-Ne possess humps in the internuclear separation range of 6–7 bohr, which is the result of repulsion with higher terms of the same symmetry. In addition, for the Ba-Ne system some excited states, e.g. $(5d)^3\Delta$ and $(6p)^1\Pi$, show a minimum near 5 bohr to which, at the present stage of calculations, we are not able to ascribe any physical meaning. The evaluated dissociation energy D_e, equilibrium position R_e and vibrational frequency ω_e for the ground state and two excited states correlated

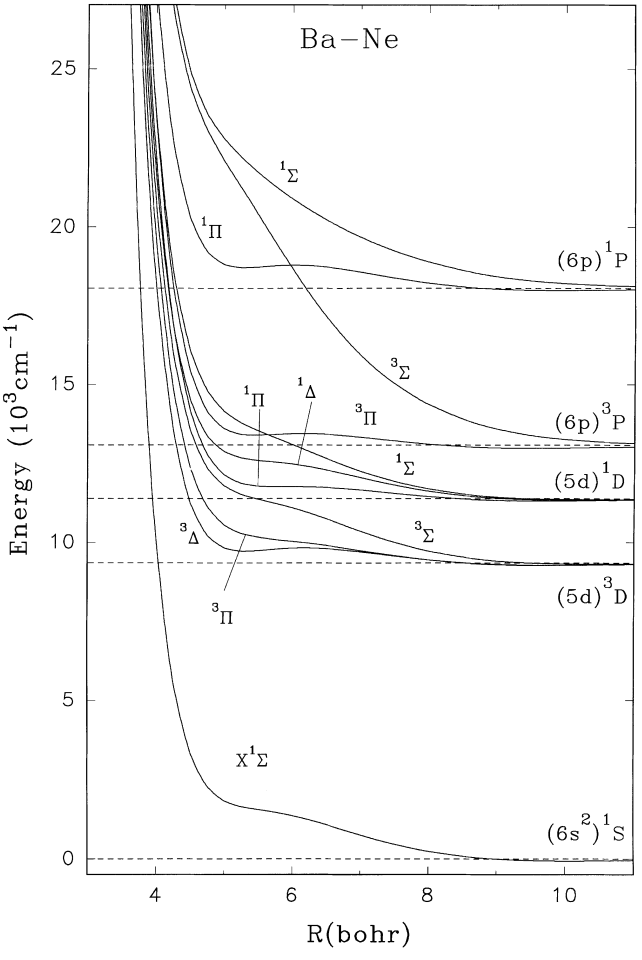

Fig. 1. Potential energy curves for the Ba-Ne system

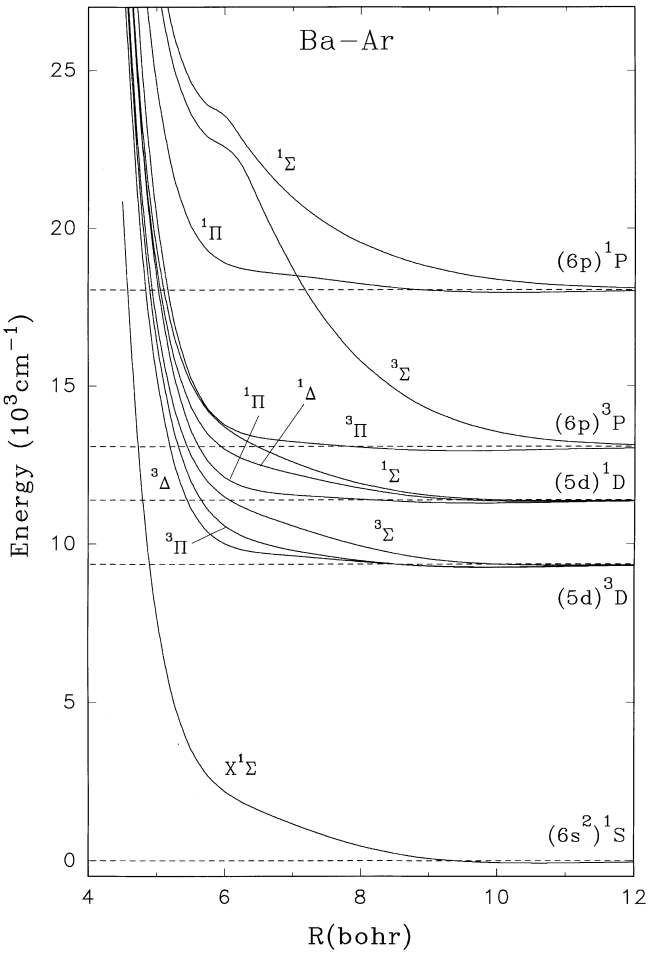

Fig. 2. Potential energy curves for the Ba-Ar system

with the resonance level of the Ba atom are compiled in Table 2. These spectroscopic parameters were derived by using a simple cubic spline approximation of the calculated potential curve near its equilibrium position. In additon, a second derivative of the potential curve was calculated numerically at R_e for evaluation of ω_e. The accuracy estimated from various choices of polynomial is better than 1 cm^{-1}, 0.1 bohr and 1 cm^{-1} for D_e, R_e and ω_e, respectively. In view of the approximations used in the present calculations, claim for a higher accuracy seems unjustified. As a result, all the dissociation energies increase with increasing mass of the RG atom. Concerning the equilibrium positions, they also slightly increase for the ground and $A^1\Pi$ states and decrease for the $B^1\Sigma$ state with the perturber mass. The evaluated very weak $B^1\Sigma$ potential minima positioned at relatively large internuclear separations result in extrema (minima) of the corresponding $B^1\Sigma - X^1\Sigma$ difference potentials which, according to the quasistatic theory of spectral line shape, give rise to red satellites in the Ba resonance line located at 8, 12, 15 and 23 cm^{-1} from the line centre, respectively, for Ba-Ne, Ba-Ar, Ba-Kr and Ba-Xe. Such red satellites were observed experimentally by Harima et al. [2] for Ba-Ar, Ba-Kr and Ba-Xe, respectively, at detunings 13 ± 5, 24 ± 5 and 45 ± 5 cm^{-1}

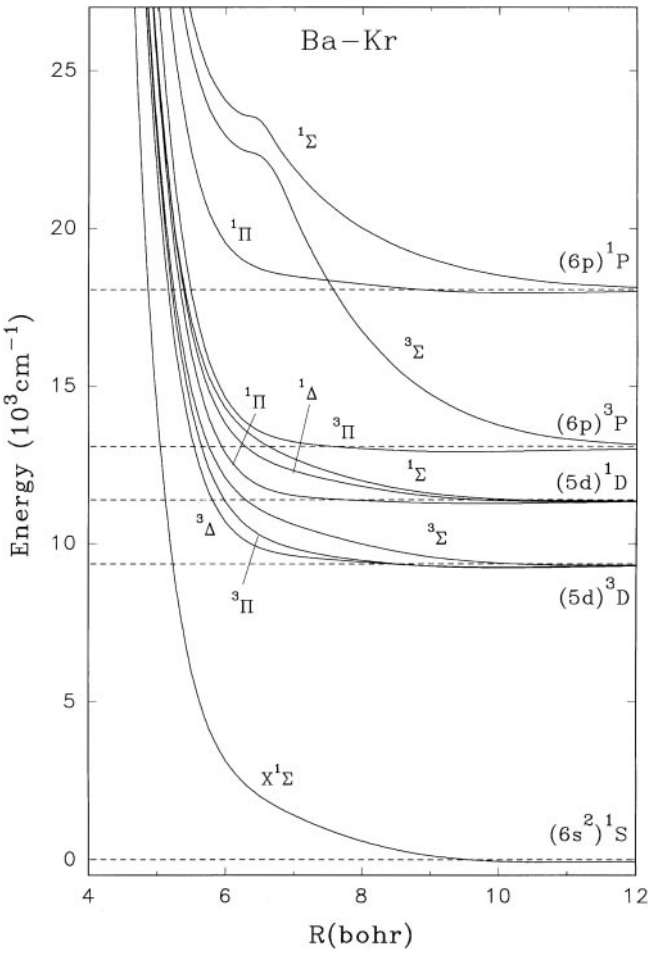

Fig. 3. Potential energy curves for the Ba-Kr system

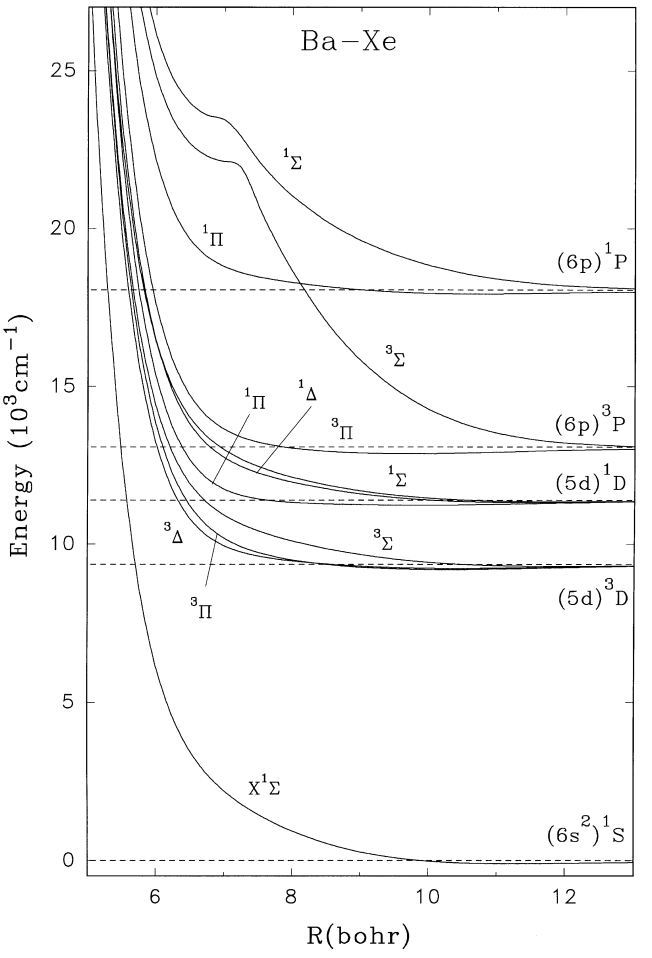

Fig. 4. Potential energy curves for the Ba-Xe system

Table 2. Spectroscopic parameters D_e (cm^{-1}), R_e (bohr) and ω_e (cm^{-1}) of the $X^1\Sigma$, $B^1\Sigma$ and $A^1\Pi$ potential curves for Ba-rare gas molecules

Molecule	$X^1\Sigma$			$B^1\Sigma$			$A^1\Pi$		
	D_e	R_e	ω_e	D_e	R_e	ω_e	D_e	R_e	ω_e
Ba-Ne	64	10.1	22	8	20.3	3	68	9.9	23
Ba-Ar	73	10.5	16	12	20.0	3	90	10.2	16
Ba-Kr	80	10.8	13	15	18.2	2	104	10.3	12
Ba-Xe	101	11.2	11	23	17.0	2	130	10.7	11

from the line centre. The minima of the $(6p)^3\Pi$ potential curves are located approximately at $R_e = 9.5$ bohr for all the Ba-RG pairs, but their depth D_e increases with increasing mass of the perturber and amounts to 98, 140, 167 and 213 cm^{-1}, respectively, for Ba-Ne, Ba-Ar, Ba-Kr and Ba-Xe. On the other hand, the $(6p)^3\Sigma$ potential curve exhibits a very shallow minimum at larger internuclear separations characterized by $D_e = 7$ cm^{-1} at $R_e = 20$ bohr, $D_e = 9$ cm^{-1} at $R_e = 19$ bohr, $D_e = 11$ cm^{-1} at $R_e = 18$ bohr, and $D_e = 22$ cm^{-1} at 15.5 bohr, respectively, for Ba-Ne, Ba-Ar, Ba-Kr and Ba-Xe. The potential curves associated with the $(5d)^3$D and $(5d)^1$D Ba levels bahave, in general, in a similar way as those correlated with the P terms. As expected, the Σ potential curve is the most repulsive. For larger internuclear separations the Π potential curve is slightly deeper than the corresponding Δ curve. This ordering is, however, reversed at shorter R range for the triplet state of all Ba-RG pairs. Unfortunately, to our knowledge, there are no experimental values of the spectroscopic parameters D_e and R_e for the Ba-RG systems in the literature to directly compare with our results.

The present potentials for Ba-Ne have been used in fully quantum close-coupling calculations of the absorption profile for the $(6s^2)^1\text{S} \rightarrow (6p)^1\text{P}$ Ba transition [26]. The absorption coefficient is defined as

$$K(\Delta\omega) = \frac{\langle \sigma(\Delta\omega) v \rangle}{\phi} \text{ cm}^5 \qquad (10)$$

where the total radiative scattering cross-section $\sigma(\Delta\omega)$ is given by

$$\sigma(\Delta\omega) = \frac{\pi}{k_0^2}\sum_{bJ_0l}(2J+1)|S^{\mathrm{J}}_{\omega}(jlJ \leftarrow j_0 l_0;\epsilon_0)|^2 \qquad (11)$$

with $J = J_0 + b$ and $b = 0, -1$ and 1, respectively, for the Q, P and R branches. Here $\Delta\omega = \omega - \omega_0$ stands for a detuning from the line centre, $\hbar\omega_{\mathrm{L}}\phi$ is the laser power, $\mathbf{k}_0$ is the wavevector of the relative motion of colliding atoms in an initial channel, j_0 and j are quantum numbers of the total electronic angular momentum $\mathbf{j}$, respectively, in the initial and final channel and v is relative collision velocity. The angular brackets in Eq. (10) denote an average over the thermal velocity distribution. The relevant closed-coupled equations are solved numerically for a given choice of relative kinetic energy ϵ_0, $\Delta\omega$ and initial total angular momentum J_0 for permitted values of b and orbital angular momentum of the nuclear motion with a quantum number l to get the five corresponding radiative S-matrix elements in terms of which the cross-section $\sigma(\Delta\omega)$ is expressed. The relative absorption coefficient $K(\Delta\omega)$ calculated for Ba-Ne is depicted in Fig. 5, where it is multiplied by $(\Delta\omega)^2$ to better display the profile structure. For comparison with experiment we have also plotted the available experimental data reported by Ni et al. [10] and Maeyama et al. [27]. The calculated profile is adjusted to only one experimental point positioned on the blue side of the line centre. As seen from the figure, there exists good agreement between the theoretical profile and the experimental data in a wide range of detunings except for far line-wings where a distinct deviation occurs, particularly in the far blue-wing region. It is interesting that the theoretical profile exhibits a clear deviation from the Lorentzian shape, although the relevant difference potentials involving the excited- and ground-state potentials have no extrema. According to the quasistatic theory of spectral line shape, such extrema are responsible for the satellite structure of the appropriate line profile. This would indicate an alternative origin of the satellite structure of atomic line profiles. Figure 6 shows the corresponding absorption profile for Ba-He based on the potential curves calculated by us earlier [18]. Agreement between theory and experiment is here even better than for Ba-Ne. Finally, comparing the present singlet potential curves with the corresponding ones calculated by us earlier [17], we note an apparent discrepancy between the two sets of potentials. The reason is that terms describing the Pauli repulsion of the RG atoms were missing in the former calculations (except for Ba-He). Thus, the Ba valence electrons experienced too much attraction from the RG core and, in consequence, the calculated potentials became too deep.

The transition dipole moments as a function of R between the ground state and the excited states correlated with the $(5d)^1$D and $(6p)^1$P Ba levels have been calculated simultaneously with the interaction potentials. For illustration, we present the results for the Ba-Ar system in Table 3. The other transition moments are

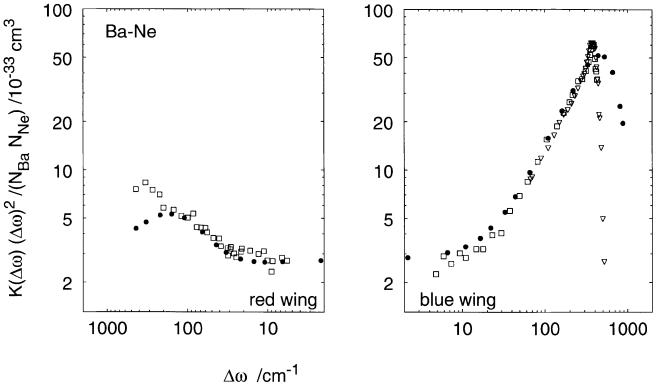

Fig. 5. Absorption coefficient calculated according to Eq. (10) for Ba-Ne: ● thermally averaged values for $T = 800$ K; □ experimental values [10]; ▽ experimental values [27]

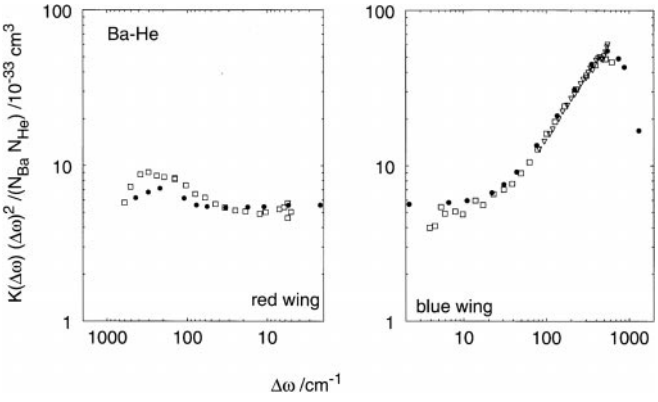

Fig. 6. Absorption coefficient calculated according to Eq. (10) for Ba-He: ● thermally averaged values for $T = 800$ K; □ experimental values [10]; ▽ experimental values [27]

available from the authors upon request. As seen from the table, the $(6p)^1\Pi - X^1\Sigma$ transition moment is nearly independent of R, whereas the $(6p)^1\Sigma - X^1\Sigma$ one decreases appreciably from its asymptotic value only at very short internuclear separations. In turn, both the transition moments to the $(5d)^1$D state increase with decreasing R and the $(5d)^1\Sigma - X^1\Sigma$ transition moment apparently predominates over the $(5d)^1\Pi - X^1\Sigma$ one. With increasing R, both the transition moments, as expected, tend to zero.

5 Conclusions

Potential energy curves and transition dipole moments for the Ba-Ne, Ba-Ar, Ba-Kr and Ba-Xe systems have been determined using pseudopotentials and polarization potentials in valence ab initio CI calculations. The results are discussed in the context of some available experimental data. It seems that the collisional effects experimentally observed in the alkaline earth atoms can be better understood in the light of these results. However, the quality of the calculated potentials as a whole can only be judged by comparison with a wider range of experimental findings.

Table 3. Transition dipole moments (au) between the ground state and the four lowest excited singlet states of the Ba-Ar system

R (bohr)	$(5d)^1\,D^1\Sigma$	$(5d)^1\,D^1\Pi$	$(6p)^1\,P^1\Sigma$	$(6p)^1\,P^1\Pi$
4.00	2.4536	2.4064	0.9285	2.4080
4.50	2.4508	1.5837	0.9806	3.0940
5.00	2.3639	0.7245	1.0434	3.4068
5.50	2.1735	0.2138	1.3405	3.4657
6.00	1.8598	0.1472	2.0775	3.4614
6.50	1.4569	0.1664	2.6588	3.4542
7.00	1.0642	0.1991	2.9634	3.4555
7.50	0.7558	0.1825	3.1373	3.4612
8.00	0.5387	0.1442	3.2402	3.4647
8.50	0.3895	0.1018	3.3048	3.4656
9.00	0.2849	0.0655	3.3483	3.4653
10.00	0.1520	0.0191	3.4025	3.4614
12.00	0.0297	0.0004	3.4463	3.4562
100.00	0.0000	0.0000	3.4545	3.4546

Acknowledgements. This work was supported by the KBN under grant No. PB1124/P03/97/12. One of us (E.C.) wishes to thank Dr. E. Paul-Kwiek for providing us with her results on the line profiles for Ba-He and Ba-Ne.

References

1. Kielkopf J (1978) J Phys B 11:25
2. Harima H, Tachibana K, Urano Y (1982) J Phys B 15:3679
3. Ehrlacher E, Huennekens J (1992) Phys Rev A 46:2642
4. Ehrlacher, E, Huennekens J (1993) Phys Rev A 47:3097
5. Kanorsky SI, Arndt M, Dziewior R, Weis A, Hänsch TW (1994) Phys Rev B 50:6296
6. Breckenridge WH, Merrow CN (1988) J Chem Phys 88:2329
7. Visticot JP, Berlande J, Cuvellier J, Mestdagh JM, Meynadier P, Pujo P de, Sublemontier O, Bell AJ, Frey JG (1990) J Chem Phys 93:5354
8. Alford WJ, Andersen N, Burnett K, Cooper J (1984) Phys Rev A 30:2366
9. Visticot JP, Pujo P de, Sublemontier O, Bell AJ, Berlande J, Cuvellier J, Gustavsson T, Lallement A, Mestdagh JM, Meynadier P, Suits AG (1992) Phys Rev A 45:6371
10. Ni SY, Goetz W, Meijer HAJ, Andersen N (1996) Z Phys D 38:303
11. Ehrlacher E, Huennekens J (1994) Phys Rev A 50:4786
12. Vadla C, Niemax K, Horvatic V, Beuc R (1995) Z Phys D 34:171
13. Brust J, Gallagher AC (1995) Phys Rev A 52:2120
14. Namiotka RK, Ehrlacher E, Sagle J, Brewer M, Namiotka DJ, Hickman AP, Streater AD, Huennekens J (1996) Phys Rev A 54:449
15. Paul-Kwiek E, Czuchaj E (1997) Mol Phys 91:113
16. Brust J, Greene CH (1997) Phys Rev A 56:2013
17. Czuchaj E, Rebentrost F, Stoll H, Preuss H (1993) Chem Phys 177:107
18. Czuchaj E, Rebentrost F, Stoll H, Preuss H (1995) Chem Phys 196:37
19. Brust J, Greene CH (1997) Phys Rev A 56:2005
20. Müller W, Flesch J, Meyer W (1984) J Chem Phys 80:3297
21. Fuentealba P, Szentpaly L von, Preuss H, Stoll H (1985) J Phys B 18:1287
22. Moore CE (1958) Atomic energy levels. (NSRDS-NBS circular no. 467) US GPO, Washington
23. Nicklass A, Dolg M, Stoll H, Preuss H (1995) J Chem Phys 102:8942
24. McMurchie L, Elbert S, Langhoff S, Davidson ER (1982) MELD program. Washington University, Seattle, USA; modified for core-polarization potentials by Wedig U, Stoll H (1984)
25. Cohen JS, Schneider B (1974) J Chem Phys 61:3230
26. Paul-Kwiek E, Czuchaj E Eur Phys J D (submitted)
27. Maeyama T, Ito H, Chiba H, Ohmori K, Ueda K, Sato Y (1992) J Chem Phys 97:9492
28. Teachout RR, Pack RT (1971) At Data 3:195
29. Lahiri J, Mukherji A (1967) Phys Rev 153:386
30. Dalgarno A, Drake GWF, Victor GA (1961) Phys Rev 176:194
31. Dalgarno A, Kingston AE (1961) Proc R Soc Lond Ser A 259:424
32. Doran HB (1974) J Phys B 7:558